Surface Science 753 (2025) 122652

Contents lists available at ScienceDirect

Surface Science

journal homepage: www.elsevier.com/locate/susc

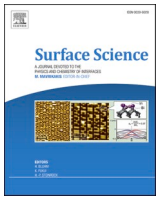

Graphene on Ni surfaces: A personal journey

Cristina Africh [a], Maria Peressi [b,*], Giovanni Comelli [a,b]

[a] CNR - Istituto Officina dei Materiali (IOM), S.S. 14 Km 163.5, Basovizza, Trieste 34149, Italy
[b] Physics Department, University of Trieste, via A. Valerio 2, Trieste 34127, Italy

ARTICLE INFO

Keywords:
Graphene
Supported graphene
Chemical vapour deposition
Scanning tunneling microscopy
Density functional theory
Ab-initio simulations

ABSTRACT

We present a short review of the work we have performed over the last decade in the framework of a scientific program dedicated to characterizing the structure, formation and functionalization of graphene layers grown on Ni surfaces. To this aim, several surface science experimental tools were complemented by numerical simulations mainly based on *ab initio* methods. In a step-by-step process, both the details and the general trends characterizing the investigated systems became progressively clearer, delineating a unique and consistent story.

All together the outcome of this intense effort can be regarded as a good example of the level of understanding of a complex problem it is possible to reach through a persistent and systematic approach in which state-of-the-art methods are employed.

Introduction

In 2004, A. Geim and K. Novoselov succeeded in preparing and identifying single-layer graphite [1], i.e. the two-dimensional arrangement of carbon atoms named graphene by an earlier study [2]. This breakthrough was recognized by the 2010 Nobel Prize in Physics, and has attracted an extraordinary and still ongoing interest worldwide by the research community, leading to an exceptional number of publications regarding this new material. An idea of the dimensions of this incredible effort can be deduced by the number of scientific papers published since 2004 which include the word “graphene” (GR) in their title, exceeding 170.000 according to Clarivate Web of Science.

Since the very beginning, the surface science community has taken an important part in this enterprise, for two main reasons. On the one hand, it became immediately obvious that “graphitic carbon” layers typically obtained on metal substrates in many earlier surface science experiments were nothing else but GR [3]; on the other hand, this community had at its disposal a wealth of sophisticated experimental and theoretical tools, perfectly adequate for preparing, functionalizing and characterizing this new material, and was thus ready to join the race.

At that time, our lab, jointly established by the University of Trieste and the Italian National Research Council, had reached a recognized level of competence in using scanning tunneling microscopy (STM) for characterizing the structure and reactivity of surfaces [4]. Still, our involvement in this topic took place only few years later, when we were asked by some colleagues in Trieste to collaborate with our expertise to their study concerning the behavior of metal nanoclusters grown on an epitaxial GR layer [5]. This first work made us fully aware of the potential of STM for this kind of studies, definitively attracting our attention to the topic and making us ready for the next step.

Soon later, a group from UK, interested in characterizing the formation and evolution of GR layers on Ni substrates - with a specific attention to possible practical applications - contacted us with the hope that STM could provide a clearer description of the structure and mechanisms involved in the GR growth process, whose clarification was proving much more complex than expected. We got fully involved in the project, based at the time only on experiments, and succeeded in providing an extremely detailed representation of the process in a publication that attracted considerable interest from the scientific community [6]. Still, the complexity of the phenomena that we observed in this occasion made it clear to us that, if we wanted to continue our efforts in this direction, it was necessary: i) to widen the set of experimental techniques to be applied; ii) to compare the experimental results with ab initio calculations, in order to facilitate their interpretation.

It thus began a long and fruitful journey - still undergoing today - in which most of our scientific work has focused on the growth and characterization of GR on different metal surfaces.

The purpose of the present paper is not that of providing an exhaustive review of the immense work that the surface science community has dedicated to this topic over the last 20 years. A number of general reviews has already been published on the subject [7,8] and can

* Corresponding author.
E-mail address: peressi@units.it (M. Peressi).

https://doi.org/10.1016/j.susc.2024.122652
Received 13 July 2024; Received in revised form 9 November 2024; Accepted 11 November 2024
Available online 13 November 2024

be consulted to this aim. Rather, we want to summarize the main stages of our personal adventure, which constitutes a small - but in our opinion significant - piece of the impressive contribution that surface science has given to the advancement of knowledge in this field. In this sense, even the list of references we provide is by no means complete, essentially citing only the works that have a direct relevance to our specific path, without any intention of disregarding the value (in several cases much more significant!) of the contributions provided by other groups worldwide.

1. The first step

In 2012, epitaxial GR grown by CVD on Ni(111) was already a hot topic in the field, as a prototypical model system for supported GR strongly interacting with the substrate. Several post-growth characterization investigations had already revealed the possible co-existence of different carbon phases on Ni(111), including surface carbide, aligned epitaxial graphene (EG) and rotated graphene (RG) domains and even GR on top of surface carbide [9–15]. Since the beginning it was evident that the different structures observed were related to the GR formation pathway, but the growth mechanism inferred from such investigations was not clear and sometimes contradictory, because a direct view on this process was missing. Also, the reproducibility of the CVD process was limited because of the strong effect of many factors not easy to control, such as the high carbon solubility in Ni and the resulting subsurface reservoir in the substrate, combined with the vast CVD parameter space [16,17]. Again, a step forward towards the engineering of reproducible growth protocols was calling for a direct investigation of the underlying atomistic mechanisms.

We investigated GR growth on Ni(111) at the nanoscale, by acquiring time series of STM images at elevated temperature (400–600 °C) while exposing the metal substrate to ethylene at low pressure (up to 10^{-6} mbar regime) [6]. We spanned wide ranges of CVD parameters and clarified that several competing mechanisms contribute to the growth process, with weights that depend not only on external factors, e.g. the substrate temperature, but also on the level of carbon pre-contamination, i.e. the amount of carbon atoms already stored in the metal subsurface before the GR growth. As shown in Fig. 1, and explained in detail in ref. [6], the overall process can be schematized as proceeding along three possible main routes: (i) in case of high C pre-contamination of the substrate, within the whole spanned temperature range, as soon as the growth temperature is reached, GR seeds are readily formed by C segregation on top of the Ni surface, followed by extension of the hexagonal network via condensation of additional C atoms at their edges, with or without ethylene exposure; (ii) for low carbon pre-contamination, at $T < 500$ °C a surface carbide layer first forms and then converts into GR via an *in-plane* or a *two-layer* mechanism; (iii) in case of low carbon pre-contamination but at $T > 500$ °C, C atoms popping up from the subsurface eject Ni surface atoms, leading to the formation of GR flakes embedded in the topmost metal layer.

Different mechanisms lead also to different GR phases: Routes (i) and (ii) result in the formation of GR layers aligned with the closed-packed lattice directions of the substrate (see Fig. 2a), while route (iii) can result in the co-existence of EG and RG domains (Fig. 2b). The latter is characterized in STM images by the appearance of a moiré pattern with variable periodicity, depending on the rotation angle, and in low energy electron diffraction (LEED) patterns by the presence of arches of extra-spots in between the hexagonal distribution of the spots due to the Ni surface atoms and to C atoms in aligned domains, respectively. Upon cooling from growth temperature to RT, nothing changes for EG domains. Underneath RG domains, instead, an interfacial surface carbide layer is formed by the segregation of further carbon atoms from the metal near-surface layers. In STM images (Fig. 2c), the RG / surface Ni carbide / Ni(111) structures can be clearly identified, as previously

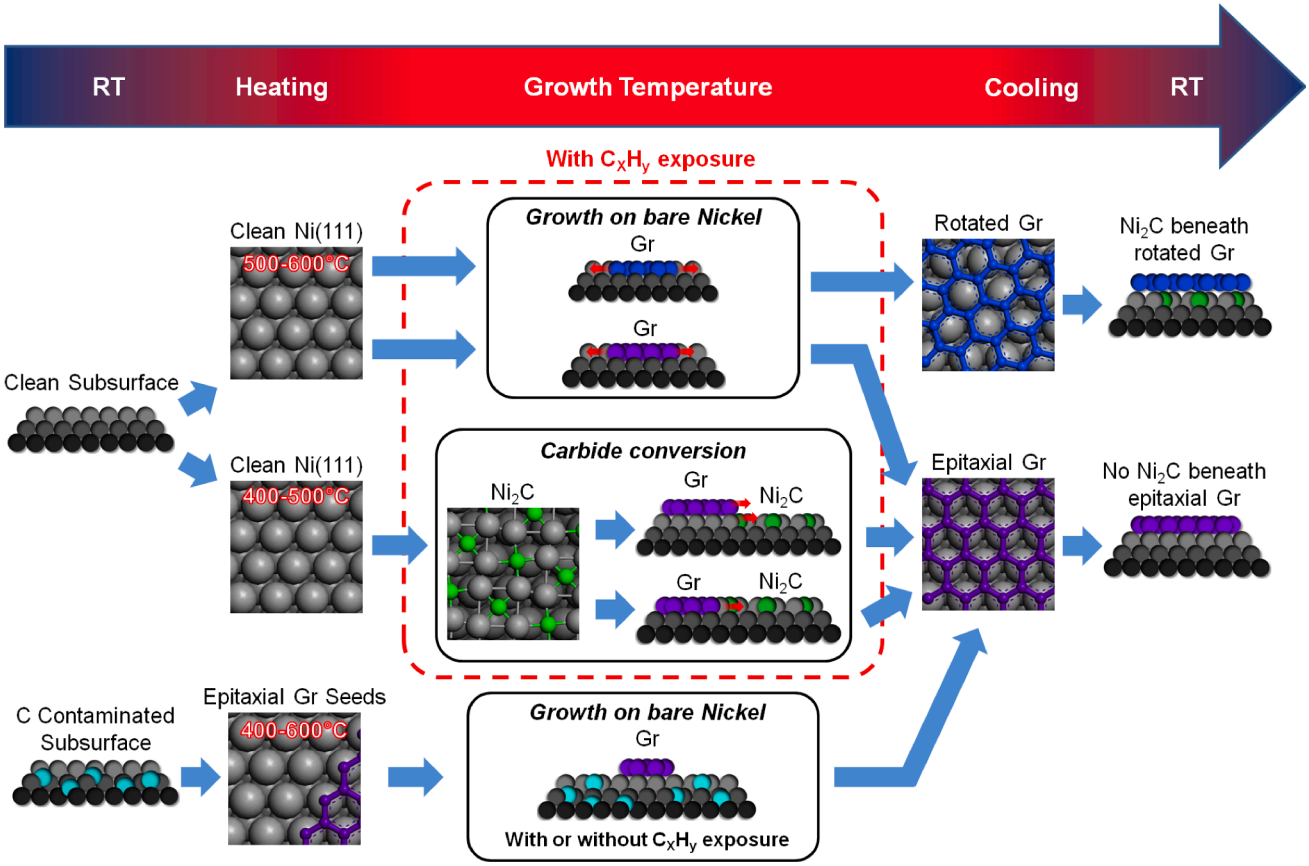

Fig. 1. Graphene growth routes on Ni(111). Reprinted with permission from [6]. Copyright 2013 American Chemical Society.

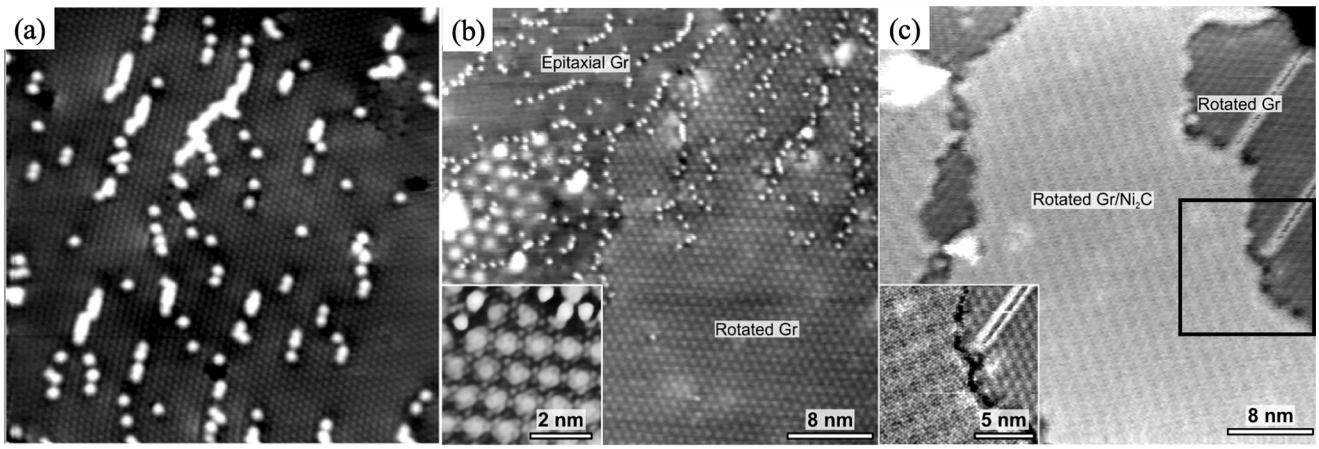

Fig. 2. Possible graphene phases on Ni(111): (a) aligned epitaxial graphene – EG; (b) rotated graphene – RG; (c) rotated graphene on top of surface nickel carbide – RGC. Adapted with permission from [6]. Copyright 2013 American Chemical Society.

nicely demonstrated in ref. [11]. Furthermore, the decoupling from the Ni substrate does not allow the stress to be accommodated in a planar configuration, due to the different thermal expansion between GR and metal, which is rather relaxed through the formation of wrinkles.

A striking feature in our STM images of GR/Ni(111), regardless of the growth route and of the match with the substrate, is the presence of randomly distributed bright spots, with the apparent dimension of a single atom. On the basis of our STM time series, we could relate their appearance with the growth process and tentatively assign them to single Ni atoms trapped in the GR mesh. The definite identification of these features, their atomic configuration and their role is further discussed in Section 6.

2. Theory sets in

This first work of some of us [6], entirely experimental, provided an extremely detailed description of the GR growth mechanism on Ni, but, as already mentioned in the Introduction, the complexity of the picture that was gradually emerging clearly indicated the need to compare the experimental data acquired with theoretical calculations from first principles that would facilitate their interpretation.

The lattice constant of the Ni(111) surface is very close to that of GR, allowing for epitaxial growth of large domains aligned with the closed-packed lattice directions of the substrate. Even for those domains, the atomic structure was not immediately clear, with alternative high-symmetry configurations previously proposed in the literature as the most stable ones [12,18–22]: i) bridge-top, with the C—C bond residing on top of a surface Ni atom like a bridge and the C atoms adsorbed equivalently off-center; ii) top-fcc (top-hcp) geometry, with one carbon atom adsorbed at the on-top position and the other on the hollow-fcc (hollow-hcp) site; iii) hcp-fcc, with reference to the positions of the two types of C atoms. Theoretical investigations based on density functional theory (DFT) did not help immediately to reach a general consensus about the most stable configuration of epitaxial graphene on Ni(111). Calculations performed within the local density approximation (LDA) or using the generalized-gradient approximation (GGA) with the Perdew-Burke-Ernzerhof (PBE) exchange-correlation functional with or without including van der Waals (vdW) interactions gave different results. Van der Waals (vdW) interactions soon emerged as an essential ingredient responsible for the binding of GR to Ni: in fact, at variance with LDA, PBE calculations without vdW correction resulted mostly in unbound configurations. In 2011 Zhao et al. [12] reported on two coexisting structures of GR on a Ni(111) surface, namely bridge-top and top-fcc, almost energetically equivalent but characterized by different experimental C 1s peaks in the x-ray photoemission spectra (XPS), with core level shifts of the different carbon atoms well reproduced by DFT.

Our first joint experimental-theoretical contribution came at this point, when, despite these advances and some consensus reached on the high symmetry structures as the lowest energy ones, their stability and ordering in energy were still under debate. Moreover, a direct microscopic experimental evidence for the coexistence of all proposed structures and an atomic level description of their transition regions were still missing. To clarify the overall picture of the different configurations of EG coexisting on a Ni(111) single crystal we used STM and DFT-GGA calculations including vdW correction, a level of theory that proved adequate and that we then always used in subsequent studies. We confirmed that top-fcc, top-hcp, and top-bridge are all stable chemisorbed structures with comparable adsorption energies [23]. Furthermore, we proved, for the first time, that the three structures could be unambiguously distinguished on the basis of their different appearance in high-resolution STM images, both experimental and simulated using the Tersoff-Hamann approximation (Fig. 3). Remarkably, the relative order of the calculated adsorption energies followed that of the observed coverage of the different configuration domains: the stronger adsorption configuration (top-fcc) was indeed the most abundant, although other factors and not just thermodynamics could influence the different registry of the epitaxially grown carbon network.

3. New insight by improving STM capability

The first steps, described above, in our STM investigations of the GR layers grown on Ni(111) were accomplished by using an almost standard commercial instrument, capable of routinely acquiring one or two images per minute. This limit strongly affected the possibility of characterizing dynamical processes in real time, and specifically the growth process itself, typically occurring on a much faster time scale. The situation drastically changed after we started using for these studies the "Fast STM" module, an Add-on unit for driving commercial scanning probe microscopes at Video Rate and beyond we had just developed [24]. In particular, by comparing Fast STM images, acquired in 250 ms each by means of this new instrument, with corresponding simulated images based on DFT calculations, we could clearly show that two different kinds of GR edges exist on Ni(111), identified as *zig-zag* and Klein [25]. For both edges, at 470 °C the terminating C atoms are directly passivated by the metal substrate, through the formation of covalent C—Ni bonds (Fig. 4), at variance with what happens at RT, where the C edge atoms, most likely hydrogenated from the residual background gas, are fully detached from the substrate. This remarkable difference in the behavior observed at different temperatures indicates that care has in general to be taken when assuming that postgrowth analysis yields the real structure adopted by the GR flake during the growth process.

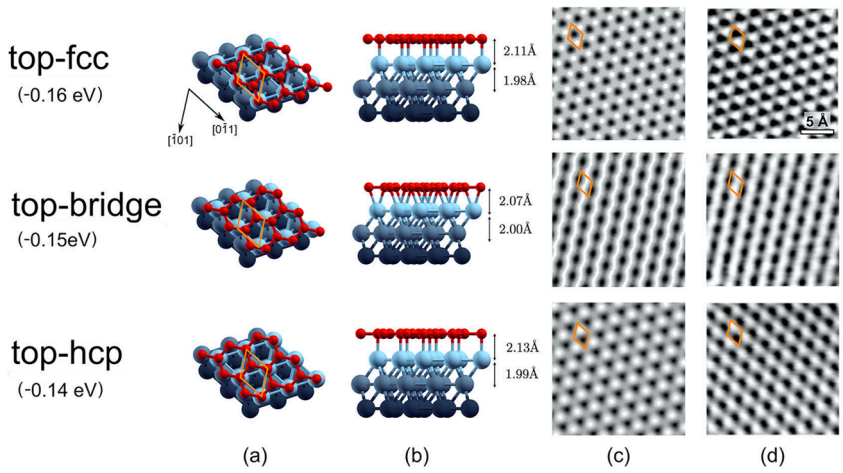

Fig. 3. Different high-symmetry configurations of GR/Ni(111). DFT optimized stick-and-ball models: top-view (a) and side-view (b) with indication of the corresponding adsorption energies. Ni atoms are progressively darker in deeper layers from the surface. Simulated (c) and experimental (d) STM images. The adhesion energy of GR on the substrate, referred to one C atom, is also reported. Adapted with permission from [23]. Copyright 2014 American Chemical Society.

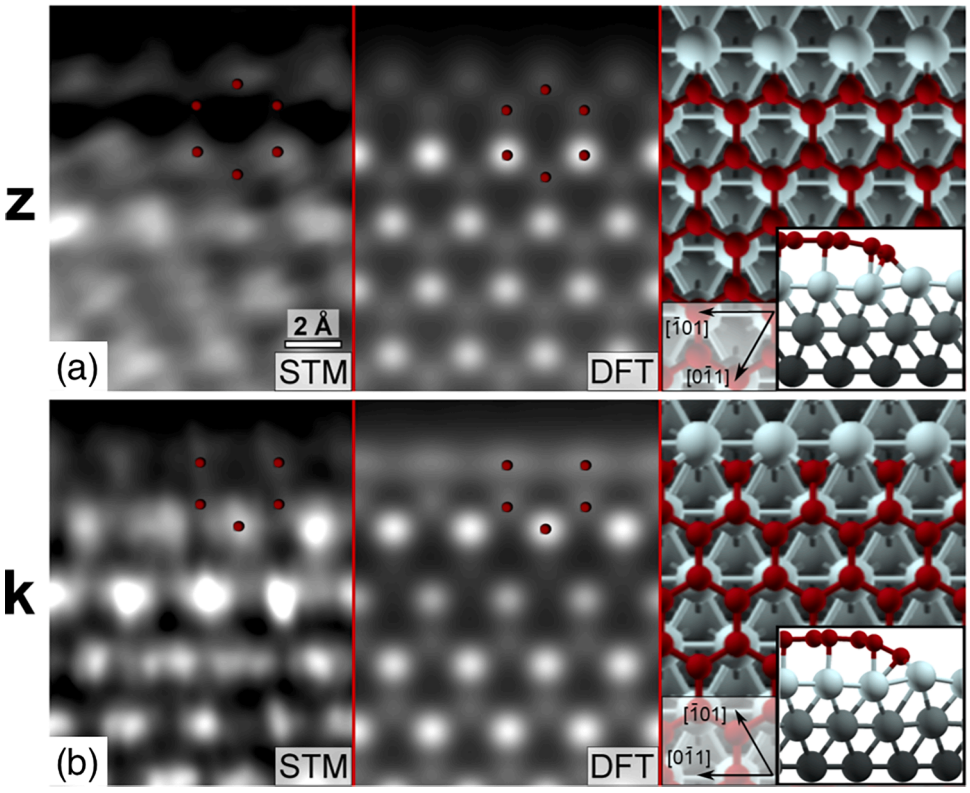

Fig. 4. Atomic structure of surface passivated (a) zig-zag and (b) Klein GR edges on Ni(111) at 470 °C. From left to right: FAST STM images, DFT-simulated images, stick-and-ball models of the DFT-optimized geometries. Red balls and dots are C atoms; gray balls are Ni atoms, darker for deeper layers from the surface. Adapted with permission from [25]. Copyright 2015 American Chemical Society.

An even more striking result was obtained few years later, when, by using the very same approach of comparing experimental Fast STM and DFT simulated images, we could reveal for the same system the crucial catalytic role played by highly mobile individual Ni atoms crossing the surface, being attracted by the kinks of the GR flake and temporarily attaching there, where they get directly involved in the growth process [26]. To capture this elusive phenomenon the STM frame acquisition time had to be pushed down to the millisecond scale and a thorough DFT analysis of several possible growth pathways had to be performed; furthermore, molecular dynamics simulations were used to prove the attraction of the diffusing Ni adatoms by the GR kink sites. Two short lived Ni adatom configurations were clearly identified, both experimentally and theoretically (Fig. 5), with DFT simulations showing that the presence of these individual Ni atoms reduces by about 35 % the height of the energy barriers involved in the GR growth process, so that they can be regarded as "single atom catalysts" [27]. Notably, during the catalytic process these wandering single Ni adatoms may remain trapped in the growing GR mesh, constituting the imaged bright spots discussed in Section 1 and 6.

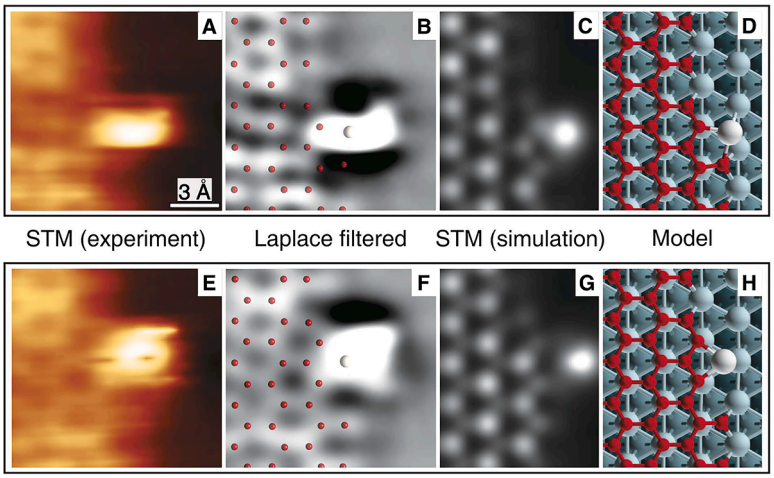

Fig. 5. Two instantaneous configurations (A-D and E-H) of Ni adatoms at the GR k-edge kinks; from left to right: selected frames from a FAST STM movie; their Laplace-filtered version with superimposed ball models; STM simulated images based on the DFT-optimized geometries. Red balls are C atoms; white and gray balls are Ni atoms, darker for deeper layers from the surface. Adapted with permission from [26]. Copyright 2018 AAAS.

4. Extending the set of experimental techniques

After having clarified the growth mechanism and the atomic structure of GR on Ni(111), we investigated the electronic structure of the different phases. To this aim, we exploited the combination of structure-sensitive low energy electron microscopy (LEEM), microprobe low energy electron diffraction (μ-LEED), energy-filtered x-ray photoemission electron microscopy (XPEEM) and microprobe angle-resolved photoemission spectroscopy (μ-ARPES) [28]. Following this approach, we were able to distinguish and investigate domains of all the three possible GR phases on Ni(111) in the same experiment, unambiguously characterizing each of them. We first of all evidenced that EG and RG, which can be clearly distinguished in LEEM, are identified in XPS by a C *1s* peak at the same binding energy BE=284.8 eV, indicating a similar interaction with the substrate regardless of the specific adsorption site. RG on a surface Ni carbide layer (labeled RGC) exhibits instead a different fingerprint in C *1s* spectra: now (i) the graphene peak is found at 284.4 eV, while (ii) a small carbide component at BE=283.2 eV confirms the presence of the interfacial layer underneath. The fact that the energy position of the RGC main peak corresponds to that of highly oriented pyrolytic graphite, already suggests a weak interaction of this GR phase with the Ni substrate. This decoupling effect in RGC was nicely confirmed by μ-ARPES measurements. As shown in Fig. 6a, in EG and RG regions the Dirac cone is shifted to 2.66 and 2.20 eV below the Fermi energy, respectively, hindering the unique electron transport properties of GR. When surface carbide is present underneath, instead, the Dirac cone at the Fermi level, and thus the semi-metal nature of GR, is restored.

As explained in Section 1, our STM experiments clearly demonstrated that GR always grows on the bare metallic Ni surface and RGC domains are just the result of additional carbon segregation underneath RG. LEEM measurements performed while heating/cooling the sample revealed that surface carbide nucleates in a well-defined temperature range, i.e. between 220° and 320 °C, and its formation is reversible. Indeed, the series of LEEM images in Fig. 6b, where darker regions are RGC, shows that temperature cycling results in regular alternation of carbon segregation to the surface (conversion of RG into RGC) and dissolution into the subsurface (which converts RGC back into RG). In turn, this is accompanied by a reversible shift in the position of the Dirac cone in μ-ARPES momentum distribution curves. By simply changing the temperature, it is thus possible to induce in GR a reversible switching between semi-metal and metal behavior. The lateral extent of the maximum switchable area corresponds to the size of the RG domain, which could span over several microns. Within this limit, the actual switched extent can be controlled by the time spent in the carbide formation/dissolution temperature window.

After the experimental investigation, we used DFT for a complete characterization of the system and to elucidate the mechanism of carbide formation, supposed to occur only underneath RG and not EG [29]. We thus built a DFT structural model for RGC with a coincidence cell between three lattices different for orientation or symmetry (Fig. 7a). For comparison, we also simulated the heterostructure with carbide grown at the interface between EG and the substrate (labelled EGC). We got a fair agreement between the calculated C *1s* core-level shift of different carbon species in RGC heterostructure and the corresponding experimental values. The density of states projected on the C atoms of GR, shown in Fig. 7b, proved the restoring of a Dirac cone in GR when carbide is formed, irrespectively on the GR orientation, and the simulated STM images in both cases resembled those of a free-standing GR layer.

DFT allowed shedding light on the C segregation process under EG and RG, yielding an estimate of the corresponding energy cost. It turned out that C enrichment of Ni outermost layers is progressively more difficult under EG: the rather strong GR/Ni interaction completely locks the nickel surface, hindering its reconstruction and thus preventing the Ni_2C formation. When GR cover is rotated with respect to the Ni(111) surface, the C binding picture changes and the density of subsurface carbon can increase up to a critical concentration which enables the structural transition of the C-enriched Ni(111) layer into a Ni_2C monolayer.

5. Exploring different Ni substrates: (100) and polycrystalline foils

5.1. Structure of the s-moiré and n-moiré GR patterns

Initially, most of the effort of the surface science community was devoted to GR grown by CVD on 3-fold close-packed surfaces of transition metal single crystals. With the aim of exploring cheaper and more common substrates, our attention progressively moved also to other surface orientations, focusing in particular on the (100), as one of the most common exposed facets of polycrystalline Ni foils and, as such, of potential interest for the scalable production and applications of GR. On the single crystal Ni(100) surface, the symmetry-mismatch between GR and the substrate (hexagonal versus square lattice) leads to different moiré superstructures according to the misorientation angle θ between the two lattices, defined as the smallest angle between one *zig-zag* direction of GR and the shortest primitive lattice vectors of the Ni(100)

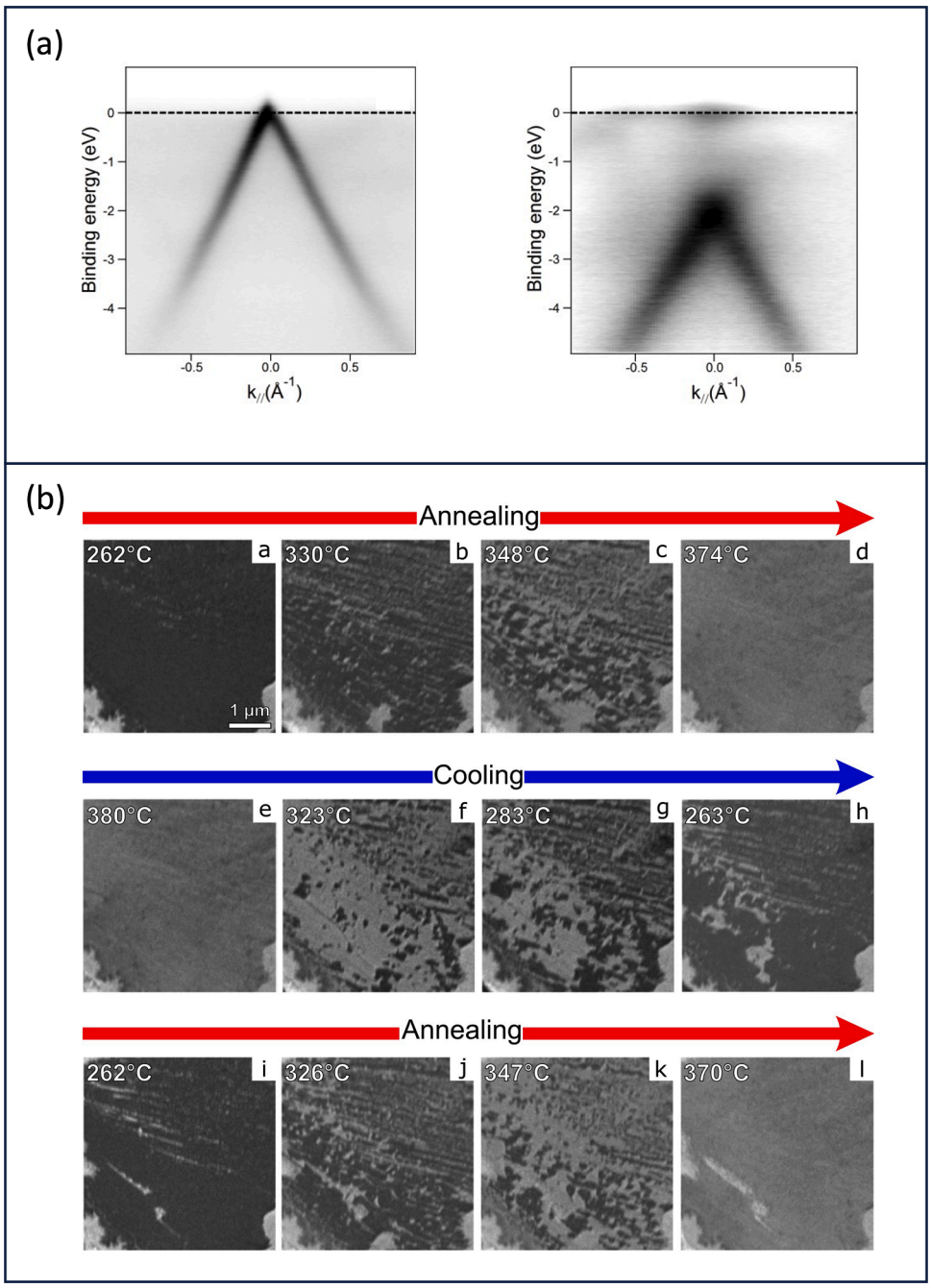

Fig. 6. Reversible decoupling from the Ni substrate: (a) Momentum distribution curves for RGC (left) and EG or RG (right); (b) effect of temperature cycling on RG domains, with the dissolution/formation of a surface Ni carbide (dark regions) underneath graphene. Adapted from [28].

surface, i.e. either the [011] or [011] direction (Fig. 8a) [30]. LEED and atomically-resolved STM allowed to precisely characterize the moiré structures, which were accompanied by a modulation of the interaction of GR with the substrate and consequently of its electronic and chemical properties.

Interestingly, we observed that one of the most common patterns corresponded to $\theta=0^{\circ}$. This can be explained by the fact that the matching between the lattice parameter of the square Ni(100) surface ($a_{Ni}^{(100)}=2.49$ Å) and the GR lattice parameter ($a_{Gr}=2.46$ Å) is excellent, allowing a 1D striped moiré (s-moiré) pattern with stripes parallel to the *zig-zag* direction and modulation along the armchair direction of GR with a period of about 15.8 Å (Fig. 8b). DFT calculations predicted a GR-substrate distance varying between 1.95 and 2.95 Å in "valleys" and "ridges", alternatively. Different misorientation angles gave rise to rhombic-network morphology moiré (n-moiré) patterns with different periodicity. For example, for the case of $\theta=11.3^{\circ}$ DFT predicted a distance from the substrate ranging from 1.95 to 2.15 Å (Fig. 8c). Notably, the height of the lowest GR regions in both s-moiré and n-moiré is comparable with that on Ni(111) [23], indicative of rather strong interfacial coupling (chemisorption), whereas in the ridges of s-moiré the GR-substrate interaction is rather weak (physisorption).

A remarkable result is that we observed the very same behavior described above to occur both on a single crystal Ni(100) surface and on polished polycrystalline Ni foils, where the predominant flat grains of Ni (100) orientations were revealed by atomically resolved images.

These GR moiré patterns were further rationalized on the basis of a simple geometric model assuming the existence of coincidence lattices. For a generic misorientation angle, a perfect commensurability between

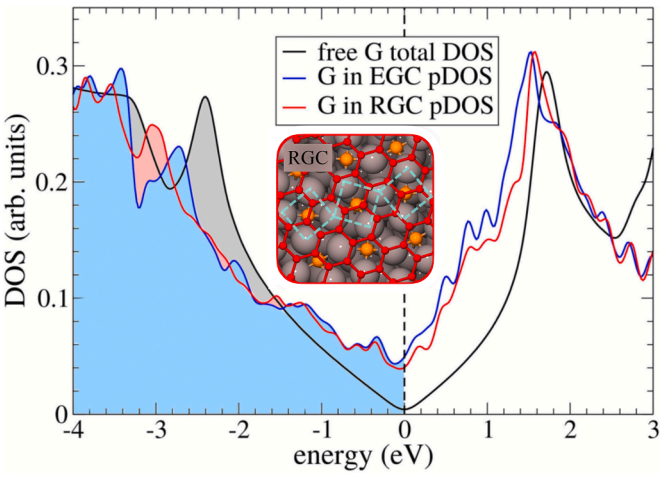

Fig. 7. GR-projected density of states (DOS) in EGC and RGC structures and in free-standing GR for comparison. Fermi levels of the corresponding structures are aligned to zero of the energy scale. In the inset: stick-and-ball model of RGC structure. Adapted with permission from [29]. Copyright 2021 American Physical Society.

the periodicity of substrate and overlayer is lacking. In order to describe a generic n-moiré with coincidence cells of reasonable size, one has to consider an approximate commensurability and a GR hexagonal lattice anisotropically slightly strained. This can be achieved either starting from the experimental observation of moiré patterns supercells [31], or by fixing the misorientation angle and predicting the smallest common supercell, within desired tolerance and size, to allow for DFT calculations with a manageable number of atoms [32]. The procedure proposed in [32] was formulated in a very general way, so that it can be applied not only to GR on Ni(100) but also to any pair of interfacing 2D lattices, such as RG on Ni(111).

5.2. GR growth mechanism on flat and stepped (100) surfaces

We applied our in-situ and in-operando approach to characterize the growth mechanisms of the layers described in the previous sub-section. Typically, upon annealing of bare Ni substrates, carbon atoms segregate to the surface from the bulk, forming a Ni_2C structure. GR grows at the one-dimensional boundary with surface Ni_2C at elevated temperatures (400–550 °C), with an orientation determined during the expansion stage by the strain at the 1D in-plane interface. Strain release appears to be the main factor governing morphology, with the interplay of two simultaneous driving forces: on the one side the need to obtain two-dimensional best registry with the substrate, via formation of moiré patterns, on the other side the requirement of optimal one-dimensional in-plane matching with the transforming Ni_2C layer, achieved by local rotation of the growing GR flake [33].

A peculiar effect was observed for the GR growth mechanism at the edges of (100) stepped surfaces of polycrystalline Ni grains [34]. When a s-moiré GR flake reaches a terrace edge of the substrate, it covers the step following a mechanism strongly dependent on its height. In particular, at step bunches, a 'staircase formation' behavior occurs, where, under the overgrowing GR, substrate terraces of equal width form (Fig. 9). This behavior was rationalized by DFT simulations, pointing to the co-existence of two competing mechanisms, related to bonding and stress: on the one side, the GR network tries to keep an optimal registry with the substrate, maximizing the number of bonds; on the other hand, this process induces in GR a progressive negative stress. On a flat surface, the balance between these opposite factors results in the corrugation of the s-stripe moiré discussed above. On a stepped (100) surface, instead, DFT predicts a minimal energy configuration formed by a series of terraces of equal width of ~2.37 nm, i.e. about 1.5 times the period of s-moiré on flat surfaces, perfectly matching the experimental observations.

5.3. Templating effect of s-moiré GR patterns: confined adsorption and GR pseudo-ribbons

GR s-moiré on Ni(100) constitutes a peculiar nanostructured 1D template on a 2D layer, confining in regularly arranged straight trails single metal atoms and few atoms clusters [35], an intriguing example of the general template role typically displayed by GR moiré on other substrates such as on Ir(111) [36,37] and Rh(111) [38]. DFT calculations showed that confined adsorption on s-moiré on Ni(100) is selective and highly dependent on the atomic species, with some species, such as Cobalt, which we investigated extensively, preferring to adsorb on

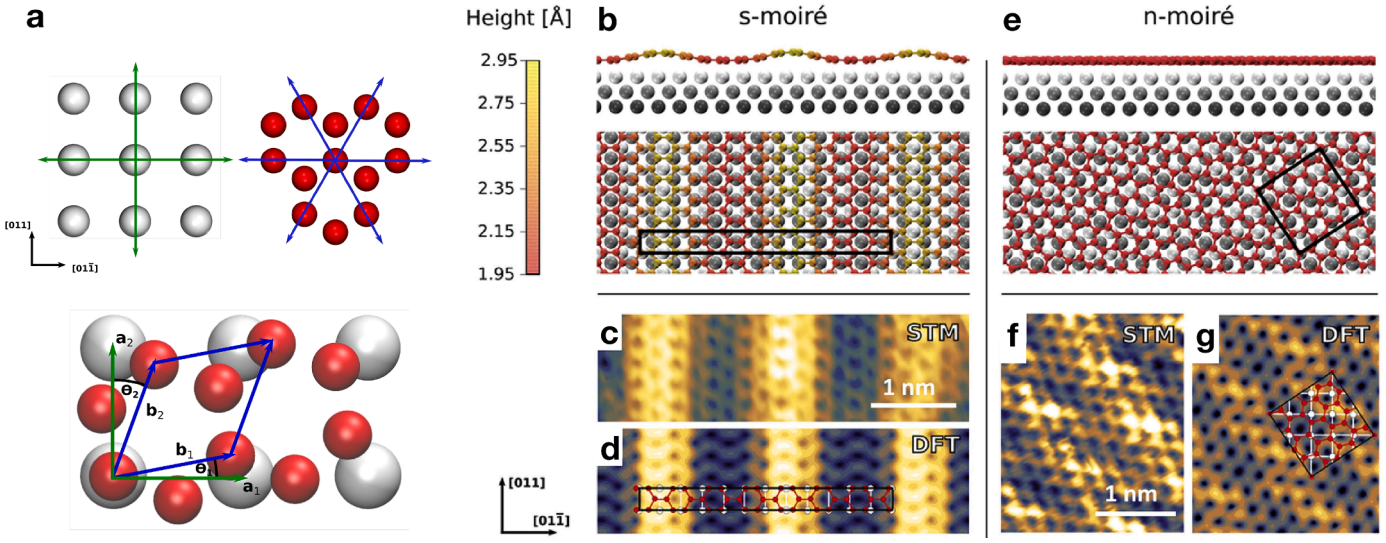

Fig. 8. Moiré patterns of GR on Ni(100). (a) Stick-and-ball models of Ni(100) surface and GR with their primitive lattice vectors ($\mathbf{a}_1$,$\mathbf{a}_2$) and ($\mathbf{b}_1$, $\mathbf{b}_2$) respectively, separately and superimposed with a misorientation angle θ. Light grey/red spheres for surface Ni and C atoms, respectively. (b-d) stripe moiré with θ=0°, (e-g) network moiré with θ=11.3°. DFT simulations (b,e) Side (upper) and top (lower) views of DFT-optimized stick-and-ball models of the two selected moiré patterns. The supercells for DFT simulation are highlighted in the top views. The color bar denotes the height of C atoms relative to the Ni surface. (c,d,f,g) Experimental (c,f) and simulated (d,g) STM images. Adapted with permission from [30]. Copyright 2018 Elsevier.

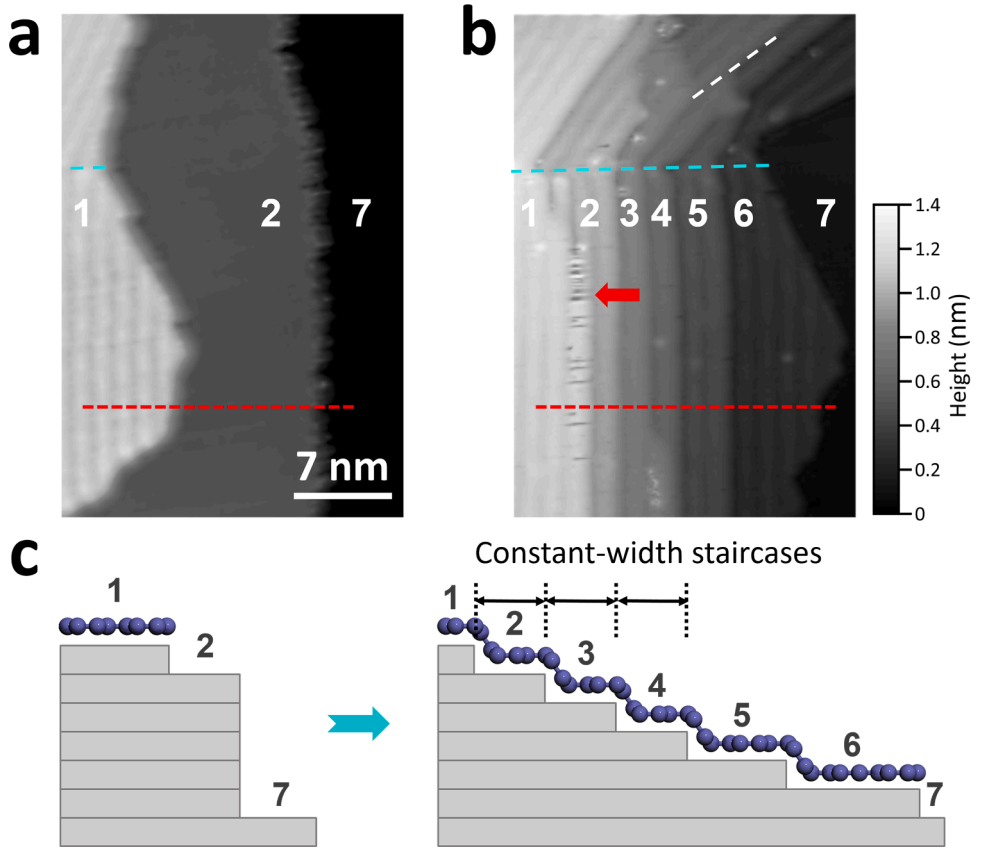

Fig. 9. GR growing at a Ni(100) step bunch: (a,b) STM images before (a) and after (b) the "staircase" formation, i.e., a series of consecutive constant-width terraces separated by monoatomic step edges. (c) Schematic models qualitatively illustrating the process (side view) along the red dashed lines in (a) and (b). The vertical direction in panels a and b corresponds to a GR misorientation angle θ=0°. Reprinted with permission from [*34*]. Copyright 2020 Elsevier.

ridges and others showing preference for valleys. The selectivity is not limited to the adsorption process only, but persists as adsorbates start diffusing, resulting in unidirectional mass transport on a continuous 2D support. No intercalation, i.e. mass transport in the "vertical" direction, was observed for this system, indicating that the GR layer protects the adsorbed atoms from dissolving into the metal substrate, similarly to the effect exerted by Ni_2C in stabilizing Co clusters on the same surface [39].

GR s-moiré constitutes also a perfect template for the formation of long, regular, ribbon-like GR structures, which we have observed and described in details [40]. By comparing microscopy/spectroscopy/diffraction experiments with numerical simulations, we explained the existence of such structures as related to the detachment of the GR layer from the substrate across two adjacent ridges of the s-moiré, as a consequence of additional C segregation. More specifically, controlled cooling of the system lead to the formation of nickel carbide underneath GR in the area delimitated by subsequent ridges, including the valley in between. The resulting structures were about 1.4 nm wide GR "pseudo-ribbons" (GPRs) with *zig-zag* edges, hundreds of nanometers long, embedded in the carbon mesh. Even though seamlessly incorporated in a matrix of strongly interacting GR, these GPRs exhibited electronic properties closely resembling those of noninteracting, quasi-freestanding 1D *zig-zag* nanoribbons. DFT simulations indicated that the GR-Ni distance increases from 1.9 to 3.3 Å in the central region of the GPR, being even larger than at the moiré ridges. The band structure projected in this region was impressively close to that of freestanding GR, specifically displaying a Dirac cone characterized by the same Fermi velocity (Fig. 10).

5.4. Simple method to characterize the GR-substrate interaction strength

Exploiting GR on Ni(100) as a prototypical system where regions with different grades of interaction with the substrate coexist, we demonstrated that I(z) spectroscopy and field emission resonance (FER) can be used as simple methods to quantitatively describe the interaction strength between graphene and a metal substrate [41]. Indeed, the tunneling current decay with tip-sample distance undergoes substantial changes when measured over a strongly or weakly interacting GR region: its exponential decay constant decreases as the GR/substrate interaction strengthens, and can range from a value close to that calculated for free standing GR (1.79 $Å^{-1}$) to about 1.1–1.2 $Å^{-1}$ for chemisorbed GR. DFT simulations allowed to rule out purely morphological effects due to the GR corrugation (i.e., curvature) and to connect this variability to the changes in the bond strength. The latter was also related to changes in the GR work function, experimentally evidenced by FER spectroscopy and calculated by DFT for the different interaction regimes.

6. GR doping and functionalization

6.1. Direct incorporation of nickel adatoms

In Section 1, reporting our seminal investigation on the growth process, we mentioned the appearance in the images of randomly distributed bright spots, tentatively assigned to single Ni atoms trapped in the GR mesh. The possible contamination of the growing GR layer by substrate atoms affects its quality; however, a controlled incorporation of Ni or other atoms in the GR mesh can be exploited as a doping method to tailor its electronic, magnetic and chemical properties. A thorough

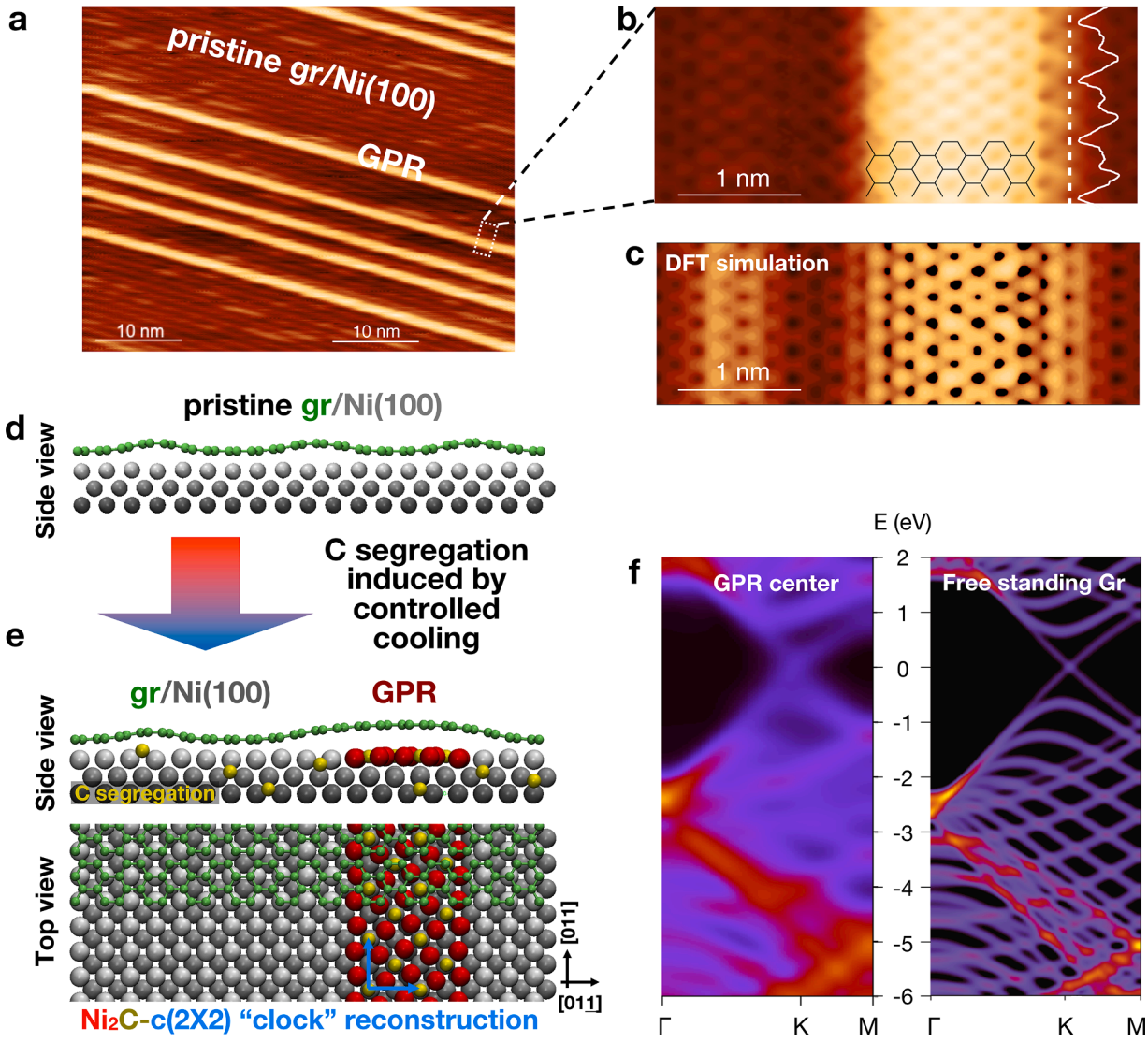

Fig. 10. GR "pseudoribbon" (GPR) on Ni(100). (a,b) STM images of a GR sheet grown on Ni(100) after cooling to room temperature, characterized by a s-moiré pattern and embedded GPR ((a): large scale image; (b): atomically-resolved zoom with a superimposed GR pattern and an intensity profile plot along the GPR zig-zag edge showing a double periodicity). (c) DFT simulated image. (d,e) Side and top view of the model structure of the GPR with a c(2 × 2) "clock" reconstruction of Ni surface underneath and formation of nickel carbide (Ni_2C). (f) Calculated band structures of the central atoms of the GPR (left) and free-standing GR (right) in the same supercell to facilitate the comparison. Adapted with permission from [*40*]. Copyright 2021 Wiley.

characterization of the observed bright spots was therefore performed.

A detailed comparison between high-resolution experimental STM images and DFT simulations of different possible structures of the defective GR on Ni(111) allowed us to precisely identify the atomic-scale configuration at the doping sites (Fig. 11), revealing that a single Ni adatom trapped into a double vacancy is the most common defect. Analysis of the electron density distribution showed that the Ni adatom is always more strongly bound to the GR layer than to the underlying substrate, thus suggesting the intriguing possibility to maintain the doping also after decoupling the layer from the substrate [42], as recently experimentally demonstrated [43].

The Ni atoms trapped in GR exhibit extremely interesting properties. First of all, their presence is observed also in GR grown on other Ni substrates, e.g. (100) and polycrystalline foils. Furthermore, they can act as anchors for adsorbed cobalt nanoaggregates, with a strong stabilization effect that prevents sintering, thus improving their efficiency for catalysis (Fig. 12) [44].

6.2. *Tuning GR doping by intercalation*

Tailoring of GR properties can be achieved not only by trapping single atoms in the GR mesh, as described in the previous section, but also through intercalation of atoms and molecules at the GR/substrate interface. As an example, we studied the effect of carbon monoxide molecules intercalated underneath a GR monolayer grown on Ni(111), showing that a CO coverage as low as 0.14 monolayer (ML) is sufficient to spatially decouple the GR mesh from the metallic substrate. The most relevant signature of the CO intercalation is a clear switch of the GR doping state, which changes from n-type in the configuration strongly interacting with the metal surface to p-type in presence of intercalated CO. The shift of the Dirac cone depends linearly on the CO coverage, reaching about 0.9 eV for the saturation value of 0.57 ML (Fig. 13). DFT predictions were compared with the results of STM, LEED and XPS, which confirmed the proposed scenario for the nearly saturated intercalated CO system. This result can open the way to the application of the GR/Ni(111) interface as gas sensor to easily detect and quantify the presence of carbon monoxide [45].

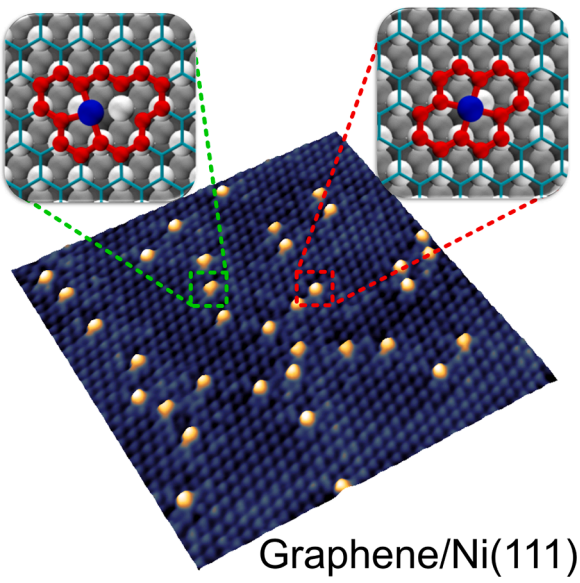

Fig. 11. Defective epitaxial graphene on Ni(111) with zoom-in on two different defects, identified as a double (highlighted by red lines) and triple (highlighted by green lines) vacancy with an individual Ni atom trapped inside. Corresponding DFT-optimized structures are shown. Adapted from [42].

An intriguing issue is the intercalation mechanism, as CO molecules would not be able to get through a perfect GR layer, which is known to be impermeable to any atomic and molecular species, except hydrogen. Regarding this point, we found that the presence of defects plays a crucial role: by means of combined experimental (STM, XPS, and LEED) and DFT simulations, we were able to elucidate in a specific case how CO molecules succeed in permeating the GR layer and get into the confined zone between GR and the Ni(111) surface. In particular, we described the role of the multiatomic vacancies passivated and stabilized by N atoms presented in the following sub-section [46].

6.3. *Nitrogen doping*

In recent years, nitrogen-doped GR layers have attracted the interest of the surface science community, with many papers dedicated to growth methods and characterization investigations [47,48]. We proposed a new, simple method to produce a flat, wide, continuous nitrogen-doped GR layer: it can be easily obtained from a nickel substrate pre-contaminated by nitrogen and then exposed to carbon-containing precursors, so that nitrogen atoms, segregating to the surface, remain trapped in the growing GR network [49]. A detailed morphological and chemical characterization was performed by combining STM and XPS measurements with DFT calculations, providing specific structural models for the various possible configurations around the nitrogen dopants.

7. Conclusions and future perspectives

The extensive and continuous work dedicated by our group to the

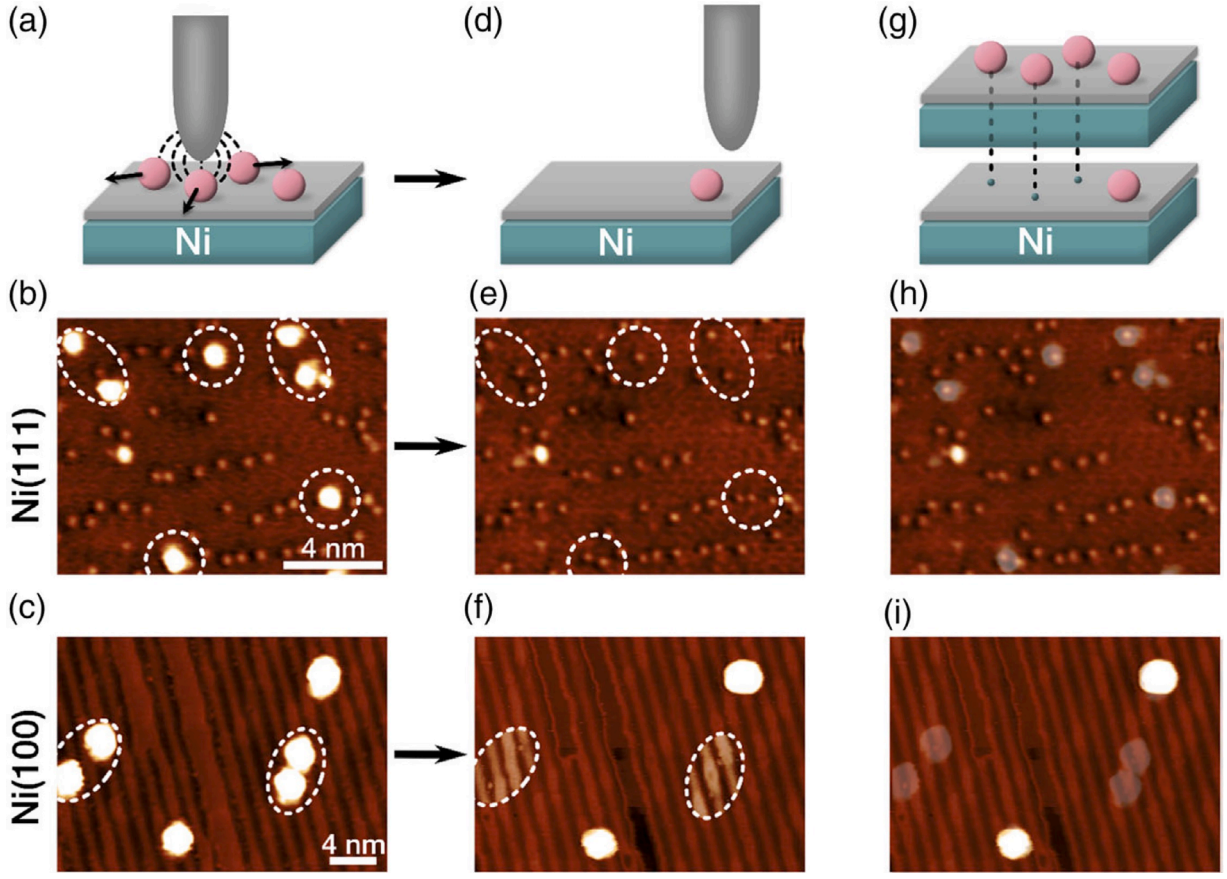

Fig. 12. Evidence of cluster adsorption site by STM manipulation. (a,d) Schematic representation of the Co clusters manipulation process. (b) STM images of Co clusters (encircled) on G/Ni(111) and (c) G/Ni(100) before manipulation. STM images of the same areas in (e,f) show the surfaces after removal of Co clusters and the respective adsorption sites, encircled and contrast adjusted in (f) for the sake of visibility of the Ni atoms. (h,i) Superposition of the STM images before and after manipulation to highlight the exact position of the removed clusters, as illustrated in scheme (g). Reprinted from [44].

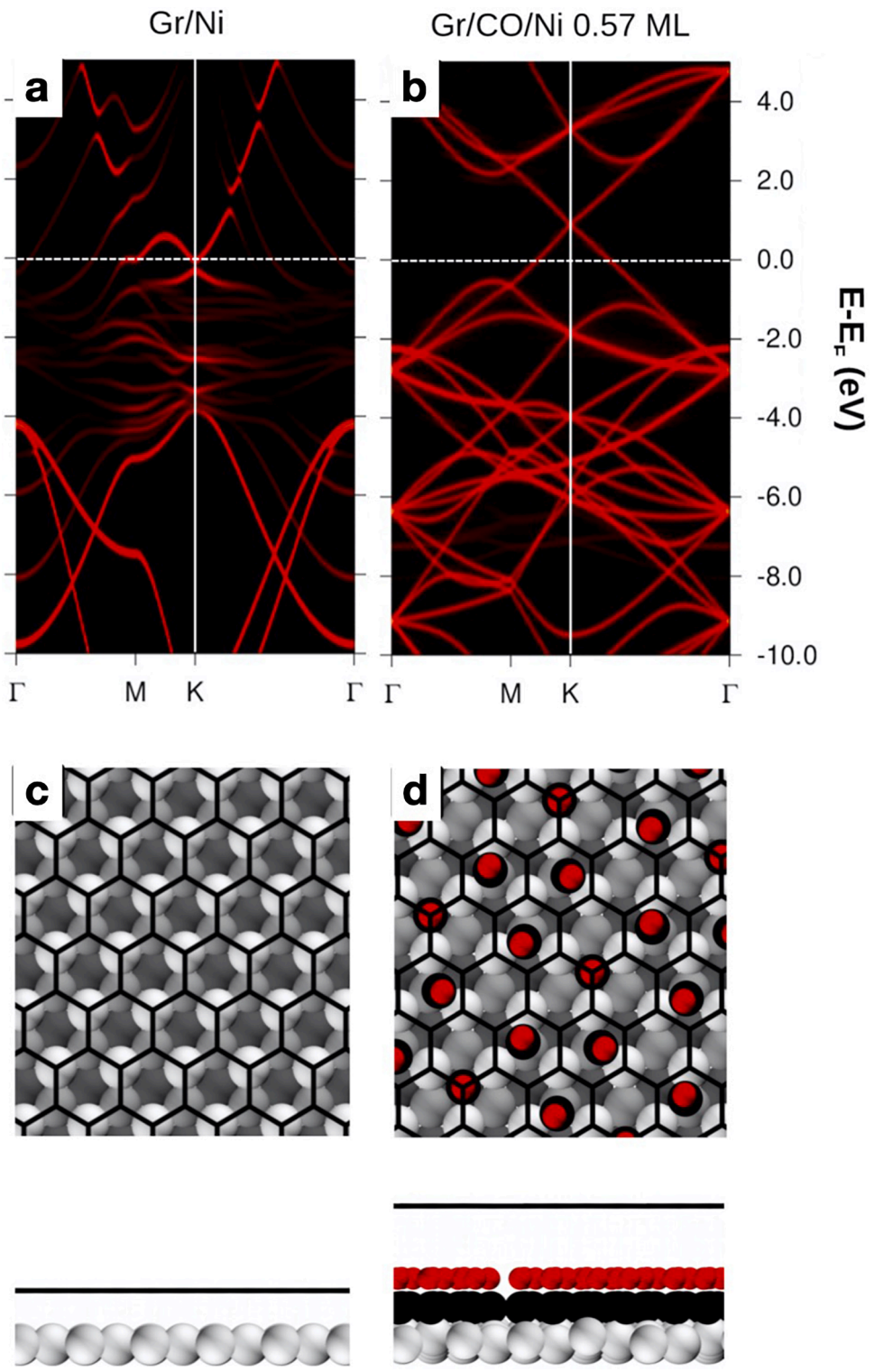

Fig. 13. Effect of CO intercalation at the GR/Ni(111) interface. (a,b) GR-projected band structure for (a) GR/Ni and (b) GR/CO/Ni (CO coverage: 0.57 monolayer), referred to the corresponding Fermi energy. For the sake of simplicity only the majority spin channel is shown. The intensity of the lines refers to the value (states (eV)) of the projected DOS. (c,d) Top (upper panels) and side (lower panels) views of the corresponding DFT-optimized models for (c) GR/Ni and (d) Gr/CO/Ni. Oxygen: red; Carbon: black (wireframe for Gr, spheres in CO); Ni: grey, darker for atoms deeper from the surface. Adapted with permission from [45]. Copyright 2020 Elsevier.

study of GR layers on Ni surfaces in more than ten years, following a systematic approach based on surface science techniques and theoretical methods, has led to a significant advancement in their characterization and comprehension. This effort has generated an overall consistent picture of the structures and mechanisms involved, providing a number and level of details which were beyond our initial expectations. It constitutes a clear example of the power that the surface science approach still has in solving complicated scientific puzzles when state of the art methods are used.

Our "journey" has not yet come to its end. Some of the strategies we

have developed in specific cases, in a series of new ongoing investigations are presently being readily extended to other systems, showing therefore a wider validity. In particular, on the one hand the "inside-out" method we proposed for N-doping is currently applied with success to other elements like B [50]; on the other end, the exploitation of the catalytic effect of single transition metal atoms for GR growth, which we first revealed for nickel, is now found to work also for cobalt, leading to Ni and Co co-doped GR layer [43] and opening the way to GR doping by many other transition metal atoms.

The large variety of novel GR based systems generated by these methods offers the opportunity to start a vast and stimulating program, aimed at characterizing in terms of chemical activity and electronic structure these new materials, with many significant prospective applications in several fields. There is little doubt that in the coming years this program will keep our attention and that of several other research groups focused.

Authors statement

G.C. and C.A. conceived and supervised the experiments. M.P. conceived and supervised the numerical simulations. All Authors discussed the results, equally contributed to the paper and approved the final version of the manuscript.

CRediT authorship contribution statement

Cristina Africh: Writing – review & editing, Writing – original draft, Supervision, Resources, Investigation, Funding acquisition, Conceptualization. **Maria Peressi:** Writing – review & editing, Writing – original draft, Supervision, Resources, Investigation, Funding acquisition, Conceptualization. **Giovanni Comelli:** Writing – review & editing, Writing – original draft, Supervision, Resources, Investigation, Funding acquisition, Conceptualization.

Declaration of competing interest

The authors declare that they have no known competing financial interests or personal relationships that could have appeared to influence the work reported in this paper.

Acknowledgement

We would like to thank all the colleagues and students who have collaborated with us in the last several years on many scientific projects based on the study of graphene; among all the others, we mention in particular Cinzia Cepek, who in 2011 has also established the original link with the English colleagues, and Cristiana Di Valentin, with whom we have established in more recent years a still ongoing collaboration regarding DFT calculations for doped GR layers.

Data availability

This is a review paper. For data/code sharing please refer to the papers of the same authors cited in this work.

References

[1] K.S. Novoselov, A.K. Geim, S.V. Morozov, D. Jiang, Y. Zhang, S.V. Dubonos, I. V. Grigorieva, A.A. Firsov, Electric field effect in atomically thin carbon films, Science 306 (2004) 666–669, https://doi.org/10.1126/science.1102896.

[2] H.P. Boehm, A. Clauss, G.O. Fischer, U. Hofmann, Das Adsorptionsverhalten sehr dünner Kohlenstoff-Folien, Z. Anorg. Allg. Chem. 316 (1962) 119–127, https://doi.org/10.1002/zaac.19623160303.

[3] R. Rosei, M. De Crescenzi, F. Sette, C. Quaresima, A. Savoia, P. Perfetti, Structure of graphitic carbon on Ni (111): a surface extended-energy-loss fine-structure study, Physical Review B 28 (1983) 1161–1164, https://doi.org/10.1103/PhysRevB.28.1161.

[4] F. Esch, S. Fabris, L. Zhou, T. Montini, C. Africh, P. Fornasiero, G. Comelli, R. Rosei, Electron localization determines defect formation on ceria substrates, Science 309 (2005) 752–755, https://doi.org/10.1126/science.11115.

[5] A. Cavallin, M. Pozzo, C. Africh, A. Baraldi, E. Vesselli, C. Dri, G. Comelli, R. Larciprete, P. Lacovig, S. Lizzit, D. Alfè, Local electronic structure and density of edge and facet atoms at Rh nanoclusters self-assembled on a graphene template, ACS Nano 6 (2012) 3034–3043, https://doi.org/10.1021/nn300651s.

[6] Laerte L. Patera, Cristina Africh, Robert S. Weatherup, Raoul Blume, Sunil Bhardwaj, Carla Castellarin-Cudia, Axel Knop-Gericke, Robert Schloegl, Giovanni Comelli, Stephan Hofmann, Cinzia Cepek, In situ observations of the atomistic mechanisms of Ni catalyzed low temperature graphene growth, ACS Nano 7 (2013) 7901, https://doi.org/10.1021/nn402927q.

[7] Matthias Batzill, The surface science of graphene: metal interfaces, CVD synthesis, nanoribbons, chemical modifications, and defects, Surf. Sci. Rep. 67 (2012) 83–115, https://doi.org/10.1016/j.surfrep.2011.12.001.

[8] Guoke Zhao, Xinming Li, Meirong Huang, Zhen Zhen, Yujia Zhong, Qiao Chen, Xuanliang Zhao, Yijia He, Ruirui Hu, Tingting Yang, Rujing Zhang, Changli Li, Jing Kong, Jian-Bin Xu, Rodney S. Ruoff, Hongwei Zhu, The physics and chemistry of graphene-on-surfaces, Chem. Soc. Rev. 46 (2017) 4417–4449, https://doi.org/10.1039/C7CS00256D.

[9] Jayeeta Lahiri, Travis S Miller, Andrew J Ross, Lyudmyla Adamska, Ivan I Oleynik, Matthias Batzill, Graphene growth and stability at nickel surfaces, New J. Phys. 13 (2011) 025001, https://doi.org/10.1088/1367-2630/13/2/025001.

[10] Jayeeta Lahiri, Travis Miller, Lyudmyla Adamska, Ivan I. Oleynik, Matthias Batzill, Graphene growth on Ni(111) by transformation of a surface carbide, Nano Lett 11 (2011) 518–522, https://doi.org/10.1021/nl103383b.

[11] P. Jacobson, B. Stöger, A. Garhofer, G.S. Parkinson, M. Schmid, R. Caudillo, F. Mittendorfer, J. Redinger, U.Nickel Diebold, Carbide as a source of grain rotation in epitaxial graphene, ACS Nano 6 (2012) 3564–3572, https://doi.org/10.1021/nn300625y.

[12] Wei Zhao, Sergey M. Kozlov, Oliver Höfert, Karin Gotterbarm, Michael P.A. Lorenz, Francesc Viñes, Christian Papp, Andreas Görling, Hans-Peter Steinruck, Graphene on Ni(111): coexistence of different surface structures, J. Phys. Chem. Lett. 2 (2011) 759–764, https://doi.org/10.1021/jz200043p.

[13] R. Addou, A. Dahal, P. Sutter, M. Batzill, Monolayer graphene growth on Ni(111) by low temperature chemical vapor deposition, Appl. Phys. Lett. 100 (2012) 021601, https://doi.org/10.1063/1.3675481.

[14] G. Odahara, S. Otani, C. Oshima, M. Suzuki, T. Yasue, T. Koshikawa, In Situ observation of graphene growth on Ni(111), Surf. Sci. 605 (2011) 1095–1098, https://doi.org/10.1016/j.susc.2011.03.011.

[15] A. Dahal, R. Addou, P. Sutter, M. Batzill, Graphene mono- layer rotation on Ni(111) facilitates bilayer graphene growth, Appl. Phys. Lett. 100 (2012) 241602, https://doi.org/10.1063/1.4729150.

[16] R. Weatherup, B. Dlubak, S. Hofmann, *Kinetic control of catalytic CVD for high quality graphene at low temperatures*, ACS Nano 6 (2012) 9996–10003, https://doi.org/10.1021/nn303674g.

[17] P.R. Kidambi, C. Ducati, B. Dlubak, D. Gardiner, R.S. Weatherup, M.-B. Martin, P. Seneor, H. Coles, S. Hofmann, The parameter space of graphene chemical vapor deposition on polycrystalline Cu, J. Phys. Chem. C 116 (2012) 22492–22501, https://doi.org/10.1021/jp303597m.

[18] G. Bertoni, L. Calmels, A. Altibelli, V. Serin, First-principles calculation of the electronic structure and EELS spectra at the graphene/Ni (111) interface, Phys. Rev. B 71 (2005) 075402, https://doi.org/10.1103/PhysRevB.71.075402.

[19] M. Fuentes-Cabrera, M. Baskes, A. Melechko, M. Simpson, Bridge structure for the graphene/Ni(111) system: a first principles study, Phys. Rev. B 77 (2008) 035405, https://doi.org/10.1103/PhysRevB.77.035405.

[20] J. Lahiri, Y. Lin, P. Bozkurt, I.I. Oleynik, M. Batzill, An extended defect in graphene as a metallic wire, Nat. Nanotechnol. 5 (2010) 326–329, https://doi.org/10.1038/nnano.2010.53.

[21] S. Kozlov, F. Viñes, A. Görling, Bonding mechanisms of graphene on metal surfaces, J. Phys. Chem. C 116 (2012) 7360–7366, https://doi.org/10.1021/jp210667f.

[22] X. Sun, S. Entani, Y. Yamauchi, A. Pratt, M. Kurahashi, Spin polarization study of graphene on the Ni(111) surface by density functional theory calculations with a semiempirical long-range dispersion correction, J. Appl. Phys. 114 (2013) 143713, https://doi.org/10.1063/1.4824186.

[23] Federico Bianchini, Laerte L. Patera, Maria Peressi, Cristina Africh, Giovanni Comelli, Atomic scale identification of Co-existing graphene structures on Ni(111), J. Phys. Chem. Lett. 5 (2014) 467, https://doi.org/10.1021/jz402609d.

[24] Friedrich Esch, Carlo Dri, Alessio Spessot, Cristina Africh, Giuseppe Cautero, Dario Giuressi, Rudi Sergo, Riccardo Tommasini, Giovanni Comelli, The fast module: an add-on unit for driving commercial scanning probe microscopes at video rate and beyond, Rev. Sci. Instr. 82 (2011) 053702, https://doi.org/10.1063/1.3585984.

[25] Laerte L. Patera, Federico Bianchini, Giulia Troiano, Carlo Dri, Cinzia Cepek, Maria Peressi, Cristina Africh, Giovanni Comelli, *Temperature driven changes of the graphene edge structure on Ni(111): substrate* vs. *hydrogen passivation*, Nano Lett 15 (2015) 56, https://doi.org/10.1021/nl5026985.

[26] Laerte L. Patera, Federico Bianchini, Cristina Africh, Carlo Dri, German Soldano, Marcelo M. Mariscal, Maria Peressi, Giovanni Comelli, Real-time imaging of adatom promoted graphene growth on nickel, Science 359 (2018) 1243, https://doi.org/10.1126/science.aan8782.

[27] Jiawen Guo, Huimin Liu, Dezheng Li, Jian Wang, Xavier Djitcheu, Dehua He, Qijian Zhang, A minireview on the synthesis of single atom catalysts, RSC Adv 12 (2022) 9373–9394, https://doi.org/10.1039/D2RA00657J.

[28] Cristina Africh, Cinzia Cepek, Laerte L. Patera, Giovanni Zamborlini, Pietro Genoni, Tevfik O. Menteş, Alessandro Sala, Andrea Locatelli,

Giovanni Comelli, Switchable graphene-substrate coupling through formation/dissolution of an intercalated Ni-carbide layer, Sci. Rep. 6 (2016) 19734, https://doi.org/10.1038/srep19734.
[29] Srdjan Stavrić, Simone del Puppo, Željko Šljivančanin, Maria Peressi, First-principles study of nickel reactivity under 2D cover: ni2C formation at the graphene/Ni(111) interface, Physical Review Materials 5 (2021) 014003, https://doi.org/10.1103/PhysRevMaterials.5.014003.
[30] Zhiyu Zou, Virginia Carnevali, Matteo Jugovac, Laerte L. Patera, Alessandro Sala, Mirco Panighel, Cinzia Cepek, German Soldano, Marcelo M. Mariscal, Maria Peressi, Giovanni Comelli, Cristina Africh, Graphene on Ni(100) micrograins: modulating the interface interaction by extended moiré superstructures, Carbon 130 (2018) 441, https://doi.org/10.1016/j.carbon.2018.01.010.
[31] Zhiyu Zou, Laerte L. Patera, Giovanni Comelli, Cristina Africh, Honeycomb on square lattices: geometric studies and strain analysis of moiré structures at a symmetry-mismatched interface, J. Phys. Chem. C 124 (2020) 25308, https://doi.org/10.1021/acs.jpcc.0c07251.
[32] V. Carnevali, S. Marcantoni, M. Peressi, Moiré patterns generated by stacked 2D lattices, Comput. Mater. Sci. 196 (2021) 110516, https://doi.org/10.1016/j.commatsci.2021.110516.
[33] Zhiyu Zou, Laerte L. Patera, Giovanni Comelli, Cristina Africh, Strain release at the graphene-Ni(100) interface investigated by in-situ and operando scanning tunnelling microscopy, Carbon 172 (2021) 296, https://doi.org/10.1016/j.carbon.2020.10.019.
[34] Zhiyu Zou, Virginia Carnevali, Laerte L. Patera, Matteo Jugovac, Cinzia Cepek, Maria Peressi, Giovanni Comelli, Cristina Africh, Operando atomic-scale study of graphene CVD growth at steps of polycrystalline nickel, Carbon 161 (2020) 528, https://doi.org/10.1016/j.carbon.2020.01.039.
[35] Srdjan Stavrić, Valeria Chesnyak, Simone del Puppo, Mirco Panighel, Giovanni Comelli, Cristina Africh, Željko Šljivančanin, Maria Peressi, *1D selective confinement and diffusion of metal atoms on graphene*, Carbon 215 (2023) 118486, https://doi.org/10.1016/j.carbon.2023.118486.
[36] Nicola Podda, Manuel Corva, Fatema Mohamed, Zhijing Feng, Carlo Dri, Filip Dvorák, Vladimir Matolin, Giovanni Comelli, Maria Peressi, Erik Vesselli, Experimental and theoretical investigation of the restructuring process induced by CO at near ambient pressure: pt nanoclusters on graphene/Ir(111), ACS Nano 11 (1) (2017) 1041–1053, https://doi.org/10.1021/acsnano.6b07876.
[37] Erik Vesselli, Maria Peressi, *Nanoscale control of metal clusters on templating supports* (Chapter 8), studies in surface science and catalysis. (Morphological, Compositional, and Shape Control of Materials for Catalysis), 1st Ed., Elsevier, 2017, pp. 285–315. Editors: P. Fornasiero and M. CargnelloISBN: 978012805090.
[38] Karin Gotterbarm, Christian Steiner, Carina Bronnbauer, Udo Bauer, Hans-Peter Steinrück, Sabine Maier, Christian Papp, Graphene-templated growth of pd nanoclusters, J. Phys. Chem. C 118 (2014) 15934–15939, https://doi.org/10.1021/jp5052563.
[39] Valeria Chesnyak, Srdjan Stavrić, Mirco Panighel, Giovanni Comelli, Maria Peressi, Cristina Africh, Carbide coating on nickel to enhance the stability of supported metal nanoclusters, Nanoscale 14 (2022) 3589, https://doi.org/10.1039/d1nr06485a.
[40] A. Sala, Zhiyu Zou, Virginia Carnevali, Mirco Panighel, Francesca Genuzio, Tevfik O. Menteş, Andrea Locatelli, Cinzia Cepek, Maria Peressi, Giovanni Comelli, Cristina Africh, Quantum confinement in aligned zigzag "Pseudo-Ribbons" embedded in graphene on Ni(100), Adv. Funct. Mater. 32 (2022) 2105844, https://doi.org/10.1002/adfm.202105844.
[41] V. Carnevali, A. Sala, P. Biasin, M. Panighel, G. Comelli, M. Peressi, C. Africh, Probing the graphene/substrate interaction by electron tunneling decay, Carbon 210 (2023) 118055, https://doi.org/10.1016/j.carbon.2023.118055.
[42] Virginia Carnevali, Laerte L. Patera, Gianluca Prandini, Matteo Jugovac, Silvio Modesti, Giovanni Comelli, Maria Peressi, Cristina Africh, Doping of epitaxial graphene by direct incorporation of nickel adatoms, Nanoscale 11 (2019) 10358, https://doi.org/10.1039/c9nr01072f.
[43] Valeria Chesnyak, Daniele Perilli, Mirco Panighel, Alessandro Namar, Alexander Markevich, Thuy An Bui, Aldo Ugolotti, Ayesha Farooq, Matus Stredansky, Clara Kofler, Cinzia Cepek, Giovanni Comelli, Jani Kotakoski, Cristiana Di Valentin, Cristina Africh, Scalable bottom-up synthesis of Co-Ni-doped graphene, Sci. Adv. 10 (2024), https://doi.org/10.1126/sciadv.ado8956.
[44] Valeria Chesnyak, Srdjan Stavrić, Mirco Panighel, Daniele Povoledo, Simone del Puppo, Maria Peressi, Giovanni Comelli, Cristina Africh, Exceptionally stable cobalt nanoclusters on functionalized graphene, Small Struct. (2024) 2400055, https://doi.org/10.1002/sstr.202400055.
[45] Simone Del Puppo, Virginia Carnevali, Daniele Perilli, Francesca Zarabara, Alberto Lodi Rizzini, Gabriele Fornasier, Erik Zupanic, Sara Fiori, Laerte L. Patera, Mirco Panighel, Sunil Bhardwaj, Zhiyu Zou, Giovanni Comelli, Cristina Africh, Cinzia Cepek, Cristiana Di Valentin, Maria Peressi, Tuning graphene doping by carbon monoxide intercalation at the Ni(111) interface, Carbon 176 (2021) 253, https://doi.org/10.1016/j.carbon.2021.01.120.
[46] Daniele Perilli, Sara Fiori, Mirco Panighel, Hongsheng Liu, Cinzia Cepek, Maria Peressi, Giovanni Comelli, Cristina Africh, Cristiana Di Valentin, Mechanism of CO Intercalation through the Graphene/Ni(111) interface and effect of doping, J. Phys. Chem. Lett. 11 (2020) 887, https://doi.org/10.1021/acs.jpclett.0c02447.
[47] R.J. Koch, M. Weser, W. Zhao, F. Viñes, K. Gotterbarm, S.M. Kozlov, O. Höfert, M. Ostler, C. Papp, J. Gebhardt, H.-P. Steinrück, A. Görling, Th. Seyller, Growth and electronic structure of nitrogen-doped graphene on Ni(111), Phys. Rev. B 86 (2012) 075401, https://doi.org/10.1103/PhysRevB.86.075401.
[48] Wei Zhao, Oliver Höfert, Karin Gotterbarm, J.F. Zhu, C. Papp, H.-P. Steinrück, Production of nitrogen-doped graphene by low-energy nitrogen implantation, J. Phys. Chem. C 116 (2012) 5062–5066, https://doi.org/10.1021/jp209927m.
[49] Sara Fiori, Daniele Perilli, Mirco Panighel, Cinzia Cepek, Aldo Ugolotti, Alessandro Sala, Hongsheng Liu, Giovanni Comelli, Cristiana Di Valentin, Cristina Africh, "Inside out" growth method for high-quality nitrogen-doped graphene, Carbon 171 (2021) 704, https://doi.org/10.1016/j.carbon.2020.09.056.
[50] Sumati Patil, Daniele Perilli, Mirco Panighel, Anu Baby, Cinzia Cepek, Giovanni Comelli, Cristiana Di Valentin, Cristina Africh, A novel synthesis route with large-scale sublattice asymmetry in boron doped graphene on Ni(111), Surface Interfaces 51 (2024) 104700, https://doi.org/10.1016/j.surfin.2024.104700.